Single-electron capture processes in slow collisions of He^{2+} ions with O_2, NH_3, N_2, and CO_2

O. Abu-Haija,[1] E. Y. Kamber,[1] S. M. Ferguson,[1] and N. Stolterfoht[2]
[1]*Physics Department, Western Michigan University, Kalamazoo, Michigan 49008, USA*
[2]*Hahn-Meitner Institut Berlin, Glienickerstrasse 100, D-14109 Berlin, Germany*
(Received 15 June 2005; published 3 October 2005)

Using the translational energy-gain spectroscopy technique, we have measured the energy-gain spectra and absolute total cross sections for single-electron capture (SEC) in collisions of He^{2+} ions with O_2, NH_3, N_2, and CO_2 at laboratory impact energies between 25 and 400 eV/amu. The measured spectra for the He^{2+}-N_2 and CO_2 collision systems show that the dominant reaction channel is due to dissociative transfer ionization (i.e., SEC accompanied by ionization of the molecular target ion). In the case of the He^{2+}-NH_3 collision system, nondissociative single-electron capture into $n=2$ states of He^+ with production of NH_3^+ in the ground state is predominantly populated. These processes are observed to be the dominant reaction channels over the entire impact energy region studied and at laboratory scattering angles between 0° and 8°. The energy dependence of total cross sections for SEC are also measured and found to slowly increase with increasing impact energies. The measured cross sections are also compared with the available measurements and theoretical results based on the Demkov and Landau-Zener models.

DOI: 10.1103/PhysRevA.72.042701 PACS number(s): 34.70.+e, 82.30.Fi

I. INTRODUCTION

Electron capture processes in low-energy ion-molecule collisions are quite interesting because they are most likely to have an impact on fields such as low- and high-temperature laboratory plasmas, and atmospheric plasmas [1,2]. In recent years, considerable attention has been directed towards the study of interaction between doubly charged helium ions and atmospheric molecules, since He^{2+} ions are the second most abundant solar wind ions in the cometary atmosphere. Observation of the He and He^+ ions in an image of comet Hale-Bopp may also be considered as a diagnostic tool in studying the interaction of the solar wind with comets [3]. In addition, electron capture processes can contribute significantly to our understanding of the observed emission spectra of He^+, N_2^+, and O_2^+ ions.

Translational energy-gain spectroscopy studies on the single-electron capture by He^{2+} ions from molecules such as N_2, O_2, NH_3, and CO_2 have been performed by several groups [4–9]. The total cross sections have also been measured by other groups [10–14]. We have recently begun a series of experiments at low collision energies, where we investigated the state-selective single-electron capture by He^{2+} ions from H_2O [15,16] and CO_2 [15]. We have also reported on the competition between dissociative and nondissociative single-electron capture in He^{2+}-O_2 collisions [17]. In this paper, we continue our studies of the electron capture by low-energy ions. Here we focus on the doubly differential cross sections, in energy and angle, and absolute total cross sections for single-electron capture in collisions of the He^{2+} ions with NH_3, N_2, O_2, and CO_2 by using translational energy-gain spectroscopy.

The data have been obtained on a differential energy spectrometer, which has been described previously by Yaltkaya *et al.* [18]. Briefly, doubly charged helium ions were produced in a recoil ion source by using 25 MeV F^{4+} ions from the Western Michigan University tandem Van de Graaff accelerator as a pump beam. An einzel lens was used to focus the ion beam extracted from the ion source into a 180° double-focusing magnet. After mass selection the ion beam was again focused by two pairs of deflectors and directed into a gas cell containing low-pressure target gas to ensure single collision conditions. Ions scattered through a nominal angle θ into a solid angle ($\Delta\Omega$) of about 3×10^{-3} sr were energy analyzed by means of a 90° double-focusing electrostatic analyzer (ESA), and then detected by a one-dimensional position sensitive channel-plate detector, which is located at the focal plane of the ESA. The scattering angle θ is selected by means of an aperture (1 mm diameter) in front of ESA.

II. THEORETICAL CONSIDERATIONS

A. Reaction dynamics

In the interaction of doubly charged helium ions with molecular targets, the following processes leading to single-electron capture can be distinguished by measuring the energy balance or gain (Q) of the reaction channel.

(i) Pure single-electron capture (SEC) (nondissociative single-electron capture):

$$He^{2+} + X \rightarrow He^+(n=2) + X^+ + Q.$$

(ii) Dissociative transfer ionization (DTI) (single-electron capture accompanied by ionization of molecular target ion):

$$He^{2+} + X \rightarrow He^+(n=1) + X^{2+} + e + Q.$$

The energy (Q) depends on the participating electronic states, masses of the projectile and target, and the laboratory scattering angle of the projectile ions. In a classical two-body collision, the translational energy of an ion undergoing inelastic scattering differs from the impact energy of the projectile ion E_o by,

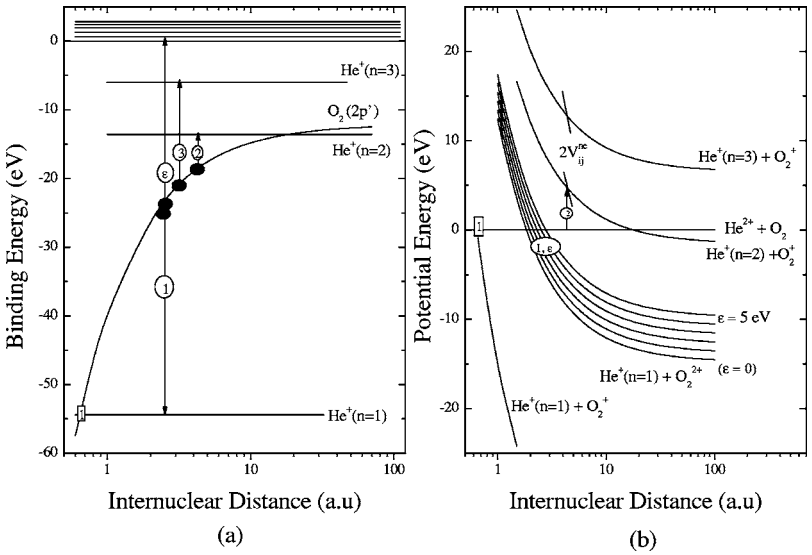

FIG. 1. (a) Correlation diagrams of molecular orbitals and (b) corresponding potential curves for the He^{2+}-O_2 system. Single-electron transitions populating the $n=1$, 2, and 3 states of He^+ ions are denoted by 1, 2, and 3, respectively. Dielectronic transitions populating the $n=1$ state and the continuum state ε are denoted as $(1,\varepsilon)$.

$$Q = E - E_o = \Delta E - \Delta K, \tag{1}$$

where ΔE is the energy defect of the reaction, and ΔK is the translational energy given to the target and is given by [19],

$$\Delta K = [(m_P/(m_P+M)\ ](1-\cos\theta_P)[(2ME_o)/(m_P+M) - \Delta E] + \{[m_P(\Delta E)^2]/(4ME_o)\}\cos\theta_P, \tag{2}$$

where m_P and M are, respectively, the projectile and target masses, and θ_P is the final laboratory scattering angle of the projectile. At low impact energies, small scattering angles, and for light projectile ions in collision with heavy targets, kinematic calculations based on classical two-body dynamics have shown that the translational energy given to the target (ΔK) is very small. Therefore, Eq. (1) reduces to $Q=\Delta E$. In the present measurements, the translational energy spectra are expressed in terms of the Q values and no correction was added to the measured energy gain.

The energy levels used in calculating the energy defect (ΔE) were taken from Moore [20] and other sources [21]. The energies (ΔE) were calculated assuming that the molecules and their product ions are in their zeroth vibrational levels. To identify the reaction channels involved, the energy-gain spectrum of the He^{2+}-Ne collision system was used as a standard to calibrate the energy scale (i.e., Q scale) for the molecular targets [4].

B. Model calculations

To interpret the experimental results, we used the model by Demkov and that by Landau and Zener. Since these models have extensively been treated in the literature [22–26], the theoretical method will only briefly be described here. Within the Demkov model [22] the transition probability from the initial state to the final state is given by

$$P_D = \exp\left(-\frac{\Delta E_c}{\alpha v_p}\right), \tag{3}$$

where v_p is the radial velocity of the projectile. The (velocity) parameter $\alpha=(\sqrt{2I_i}+\sqrt{2I_f})/2$ is obtained from the binding energies I_i and I_f of the electron in the initial and final states labeled i and f, respectively [22]. The parameter $\Delta E_c = \Delta E_{if}(R_c)$ is the energy difference between the initial and the final potential curves at the transition radius R_c. Within the Demkov model, transitions occur at the internuclear distance where the energy difference ΔE_{if} is equal to twice the coupling matrix element V_{if}. Thus, the transition radius R_c is obtained by solving the equation $\Delta E(R_c)=2V_{if}^{ne}(R_c)$. The matrix element, which couples the initial state representing the $2p$ orbital of H_2O with the final state representing the levels $n=2$ and 3 of He^+, may be approximated by [25]

$$V_{if} = 3.6\alpha^2 \exp(-0.86\alpha R), \tag{4}$$

where R is the internuclear distance.

Since the transition region is passed twice in a collision, the double passage probability is evaluated using the well-known statistical rule [25],

$$P_{if} = 2p_D(1-p_D). \tag{5}$$

The Landau-Zener (LZ) model [23,24] treats transitions at crossings of diabatic states at distance R_c. In Fig. 1(b) the region of crossings of the initial states $He^{2+}+O_2$ with various (continuum) states $He^+(n=1)+O_2^{2+}(\varepsilon)$ is labeled $(1,\varepsilon)$. The LZ model evaluates the probability p_{LZ} for the transition to remain in the initial diabatic state in a single crossing and is given by

$$p_{LZ} = \exp\left(-\frac{2\pi H_c^2}{F_c v_p}\right), \tag{6}$$

where the "force" F_c is obtained as the derivative of the energy difference ΔE at R_c. The dielectronic matrix element $H_c=H_{ij}^{ee}(R_c)$ is evaluated at R_c and v_p is the projectile velocity, as before. For dielectronic transitions, produced by the electron-electron (ee) interaction, the matrix element may be approximated by [26],

$$H_{if}^{ee} = 0.15\alpha^2 \exp(-0.86\alpha R), \tag{7}$$

where α is the velocity parameter already given in conjunction with the Demkov theory.

For $p_{LZ} \ll 1$ the probability for populating the number v of final states is obtained as $P_{if}=1-p_{LZ}^{2v}$. The unknown number of final states was set to be equal to $v=20$. For such a large number the results do not change significantly with increasing v. Therefore, the choice of v is uncritical for the transition probability. It should be noted that the dielectronic matrix elements H_{if}^{ee} is relatively small in comparison with the matrix elements V_{if} responsible for Demkov-type transitions. However, this smallness is compensated by the relative high number v of final states [27].

After evaluation of the transition probability, the corresponding cross section is obtained using a simple approximation. We recall that the transitions considered here take place at a specific distance R_c so that one may use a "geometric" expression for the cross section

$$\sigma_{if} = P_{if}(R_c)\pi R_c^2 \tag{8}$$

which implies that $P_{if}(R)=P_{if}(R_c)=\text{const}$ for $R<R_c$ and $P_{if}(R)=0$ elsewhere.

C. Correlation diagrams and capture mechanisms

From previous measurements a general trend can clearly be observed that the $n=2$ state is most effectively populated at highest energies and DTI process becomes more populated at low energies [16]. To understand the SEC and DTI processes, we used the correlation diagrams of molecular orbitals (MO) and the corresponding potential curves [16] to visualize the different capture mechanisms and to show the transition energies involved for the collision systems studied here. Figures 1(a) and 1(b) show the molecular diagram and the corresponding potential curves, respectively, for the He^{2+}-O_2 collision system.

As seen in Fig. 1(b), transitions into $n=2$ occur at distances near 4.4 a.u. (see the arrow labeled 2) initiated by mechanisms treated by the Demkov model [16,22]. Similarly, transitions into the $n=3$ level of He^+ occur at about 3 a.u. (arrow labeled 3). It should be emphasized that Demkov-type transitions occur at locations where the potential energy difference is equal to twice the interaction matrix element V_{ij} given by Eq. (4) [16]. This indicates that the He^+ ($n=2$) formation proceeds via a single-electron process governed by the nucleus-electron interaction.

The population of the $n=1$ state of He^+ occurs near R =2.5 a.u. as a result of a two-electron (dielectronic) process, where one electron is transferred into the MO correlated with the $n=1$ level and another electron is ionized. This transfer ionization (TI) process is produced by the electron-electron interaction, where the potential energy, liberated by the transition into the deeply lying $n=1$ orbital, is used to ionize another electron (the sum of potential energy changes is equal to zero) thereby resulting in fragmentation of the O_2 molecule. In Fig. 1(b), the dielectronic transitions, denoted as $(1,\varepsilon)$, occur at the locations where the incident channel $He^{2+}+O_2$ crosses a series of potential curves $He^+ + O_2{}^{2+}(\varepsilon)$. This results in the transfer of one electron of O_2 to the He^{2+} ion while a second electron is transferred into the continuum of O_2 with an energy ε.

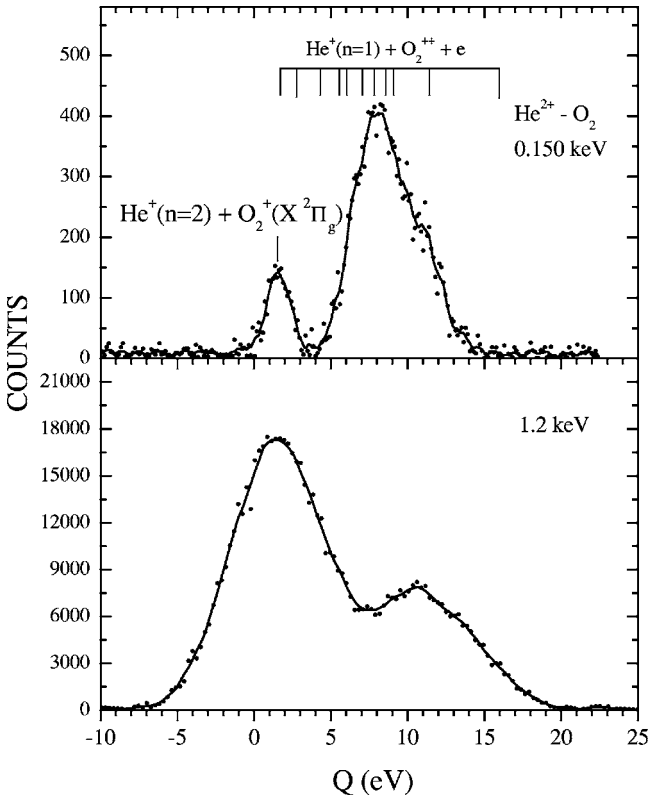

FIG. 2. Translational energy-gain spectra for single-electron capture by He^{2+} ions from O_2 at collision energies of 0.15 and 1.2 keV. Smooth lines are drawn to guide the eye.

III. RESULTS AND DISCUSSION

A. $He^{2+}+O_2$ collisions

We reported in an earlier work [17] on the competition between DTI and nondissociative SEC by He^{2+} ions from O_2 at laboratory impact energies between 0.1 and 1.0 keV. However, the absolute scales for the cross sections were evaluated by normalizing the total capture cross-section measurements of Ishii *et al.* [13]. In this work, we present new experimental results for absolute state-selective and total cross sections for single-electron capture and compared with the available measurements and theoretical calculations. For these measurements, the target gas pressure in the collision cell was measured by a capacitance manometer (MKS Baratron), and was typically $\leqslant 2$ mTorr, to ensure single-collision conditions. In addition, an angular acceptance of about $\pm 12°$ was used after removing the angular selector in front of the ESA. The total experimental uncertainties for absolute values of the total cross sections were obtained by a quadratic sum of the statistical deviations, determination of target thickness, and counting efficiency.

Figure 2 shows translational energy-gain spectra for single-electron capture by He^{2+} ions from O_2 at collision energies of 0.15 and 1.2 keV. At the collision energy of 0.15 keV, the observed spectrum is dominated by contributions from DTI, presumably due to single-electron capture into $n=1$ states of He^+ with simultaneous ionization of the target-ion product [17]. There are smaller contributions due

TABLE I. State-selective cross sections (10^{-16} cm^2) for single-electron capture by He^{2+} ions from O_2 leading to He^+ ($n=1$) and He^+ ($n=2$) formations.

Energy (keV/amu)	O_2	
	He^+ ($n=1$)	He^+ ($n=2$)
0.025	1.51±0.26	0.16±0.06
0.050	2.46±0.33	0.34±0.12
0.075	3.07±0.32	0.72±0.17
0.100	3.50±0.44	1.28±0.19
0.125	4.05±0.52	1.75±0.26
0.150	4.15±0.48	2.81±0.38
0.175	3.93±0.47	3.55±0.42
0.200	3.65±0.45	4.23±0.51
0.225	3.46±0.49	4.46±0.61
0.250	3.43±0.51	4.79±0.57
0.275	3.38±0.52	5.03±0.72
0.300	3.37±0.50	5.24±0.64
0.325	3.37±0.50	5.73±0.69
0.350	3.27±0.50	5.92±0.71
0.375		
0.400	3.12±0.46	5.89±0.78

TABLE II. Absolute total cross sections (10^{-16} cm^2) for single-electron capture by He^{2+} ions from O_2, CO_2, N_2, and NH_3.

Energy (keV/amu)	O_2	CO_2	N_2	NH_3
0.025	1.67±0.28	0.48±0.09	1.58±0.17	20.24±0.19
0.050	2.80±0.37	0.84±0.13	2.51±0.27	20.66±0.20
0.075	3.79±0.38	1.42±0.15	2.87±0.30	20.73±0.20
0.100	4.78±0.47	1.76±0.22	3.51±0.35	21.00±0.20
0.125	5.80±0.56	2.02±0.25	3.66±0.37	21.28±0.20
0.150	6.96±0.68	2.47±0.28	3.84±0.42	21.43±0.21
0.175	7.48±0.76	3.23±0.35	3.91±0.44	21.48±0.21
0.200	7.89±0.78	3.51±0.36	3.94±0.42	21.49±0.21
0.225	7.92±0.20	3.70±0.39	3.98±0.44	21.61±0.21
0.250	8.22±0.80	3.83±0.20	4.02±0.45	21.65±0.21
0.275	8.41±0.82	3.85±0.19	4.09±0.47	21.78±0.22
0.300	8.62±0.83	3.93±0.21	4.11±0.48	21.91±0.22
0.325	9.11±0.88	3.99±0.23	4.18±0.48	21.91±0.22
0.350	9.19±0.89	4.07±0.24	4.22±0.49	22.01±0.23
0.375		4.15±0.28	4.27±0.51	
0.400	9.00±0.87			

to nondissociative SEC into $n=2$ states of He^+ ions. At the collision energy of 1.2 keV, capture into $n=2$ states of He^+ ions becomes dominant and contributions from DTI channel decrease significantly [17]. The dependence of the cross-section ratio $\sigma(\mathrm{DTI})/\sigma(\mathrm{SEC})$ on the collision energy will be discussed later in this section in terms of LZ and Demkov models.

We have also measured absolute state-selective and total cross sections for single-electron capture by He^{2+} ions from O_2 at laboratory energies between 0.025 and 0.4 keV/amu. Experimental data for absolute state-selective and total cross sections, along with the relative uncertainties, are listed in Tables I and II. These cross sections, together with other experimental data and theoretical calculations obtained by the models described in detail in Sec. II B, are depicted as a function of energy in Fig. 3. The measured cross sections for capture into the He^+ ($n=1$) state increase with increasing energy, peak at a collision energy of $E=0.15$ keV/amu, and show a slightly decreasing trend at larger collision energies. On the other hand, the measured cross sections for capture into the He^+ ($n=2$) states slowly increase with increasing collision energy and become the dominant process at collision energies of $E \geqslant 0.2$ keV/amu. The increase of the probabilities for single-electron capture into the He^+ ($n=2$) states with increasing projectile energy as predicted by the Demkov model is due to the fact that the transitions are produced by dynamic coupling effects initiated by the nucleus-electron interaction, which requires kinetic energy from the collision partners. On the contrary, the cross section for dielectronic transitions leading to He^+ ($n=1$) formation decreases with increasing projectile energy.

The energy dependence of the measured cross sections (Fig. 2) for capture into the He^+ ($n=1$) state is fairly well reproduced by the Landau-Zener model at energies above 0.25 keV/amu, while capture into He^+ ($n=2$) states agrees well with the Demkov calculations. The large discrepancy between our data and the Landau-Zener model for capture into He^+ ($n=1$) at low energies can be partially explained by

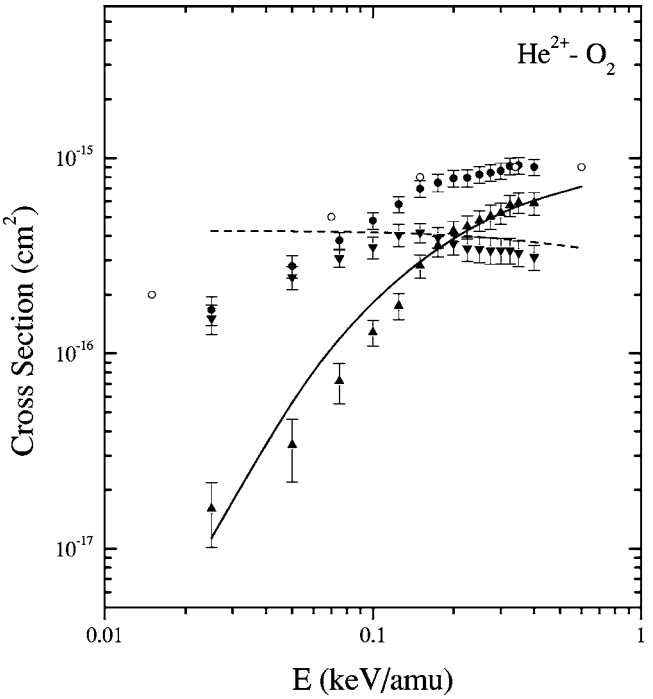

FIG. 3. Cross sections for single-electron capture by He^{2+} ions from O_2. Total cross sections: ●, present work; ○, Ishii *et al.* [13]. Capture into He^+ ($n=1$) state: ▼, present work. Capture into He^+ ($n=2$) state: ▲, present work. Theory: solid line, Demkov model; dashed line, LZ model.

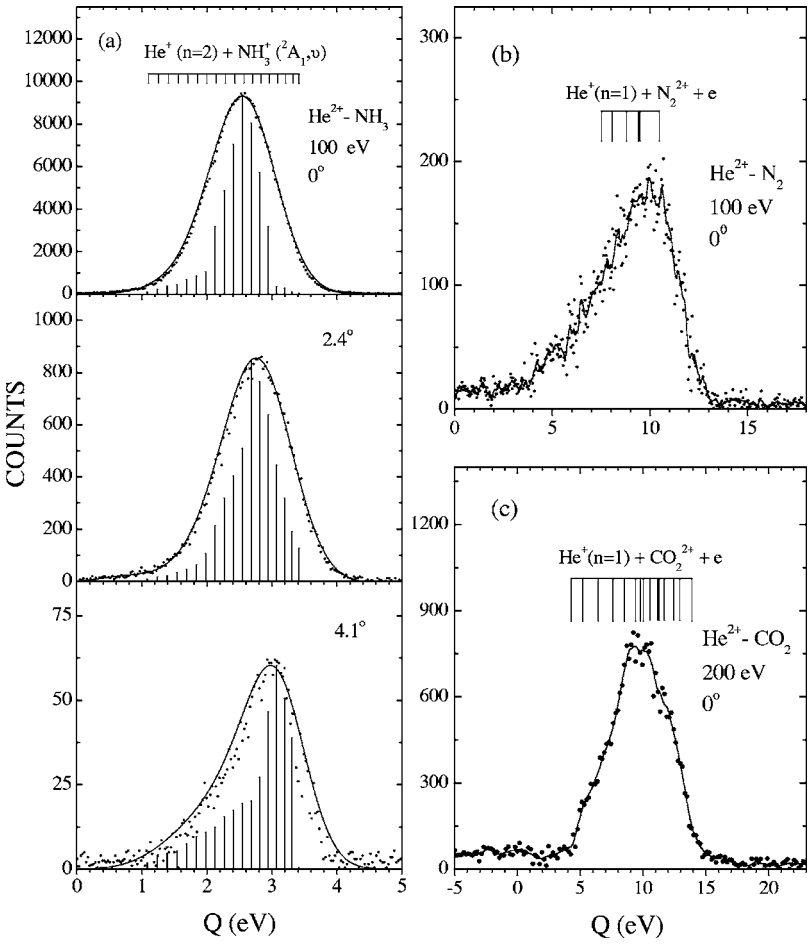

FIG. 4. Translational energy-gain spectra for single-electron capture by He^{2+} ions. (a) From NH_3 at different projectile laboratory scattering angles. The vertical lines represent the relative populations of each vibrational levels of NH_3^+ $(X\,^2A_1,v)$ ranging between $v=0$ and 17; the vertical line at the highest value of ΔE corresponds to the lowest vibrational level of the NH_3^+ product (i.e., $v=0$); (b) N_2; (c) CO_2. Spline lines are drawn to guide the eye.

the fact that the theory includes also double-electron capture channel, which is known to increase strongly with decreasing energies. Furthermore the model includes not only transfer ionization but also transfer excitation to high Rydberg states of He^+, which is also important at low energies, since it occurs at small distances where the dielectronic matrix element is enhanced. In addition, the measured total cross sections slowly increase with increasing collision energy and are lower than those of Ishii *et al.* [13] by a factor of 1.7. However, our results are in reasonably good agreement with the experimental results of Ishii *et al.* [13], at energies $\geqslant$0.125 keV/amu.

B. $He^{2+}+NH_3$ collisions

Figure 4(a) shows the translational energy-gain spectra obtained for single-electron capture by 100 eV He^{2+} ions from NH_3 at different scattering angles. At 0° scattering angle, only one peak is observed that corresponds to nondissociative single-electron capture into the $n=2$ states of He^+ with production of NH_3^+ in the ground state $(X\,^2A_1,v)$, where v refers to a vibrational state of the target product. The vertical lines on the upper part of the figure represent the calculated energy-gain values for the reaction producing NH_3^+ $(X\,^2A_1,v)$ through the process

$$He^{2+} + NH_3(X\,^1A_1, v=0) \rightarrow He^+(n=2) + NH_3^+(X\,^2A_1,v) + (3.417 - 1.082\ \text{eV}).$$

Also shown are the relative populations of each vibrational levels of NH_3^+ $(X\,^2A_1,v)$. The populations were determined by fitting Gaussian peak shapes with fixed positions and widths equal to the experimental energy resolution of 0.8 eV to the measured spectra. The value of the largest population has been normalized to the dominant peak observed in the spectrum. Comparison with the results of Fárnĩk *et al.* [7] at 70 eV shows good agreement with the present measurements. However, we were unable to resolve the vibrational states because of low-energy resolution used in our measurements. It is interesting to note that the position of the peak is centered around $v=7$ in agreement with the calculated populations [28]. As the scattering angle is increased, the relative importance of the lower vibrational levels increases and the position of the peak is relatively shifted to $v=4$ at $\theta=4.1°$.

We have also measured total cross sections for single-electron capture by He^{2+} ions from NH_3 at laboratory collision energies between 0.025 and 0.35 keV/amu. Our results are displayed as a function of collision energy in Fig. 5, together with calculations based on Demkov model. Our experimental cross-sections exhibit weak energy dependence and they are almost constant with increasing impact energy, a behavior that is attributed to availability of many capture channels, which are situated nearly at the center of the reaction window. The Demkov results lie just below the experimental results and show the same energy dependence. There are no other experimental data available for comparison.

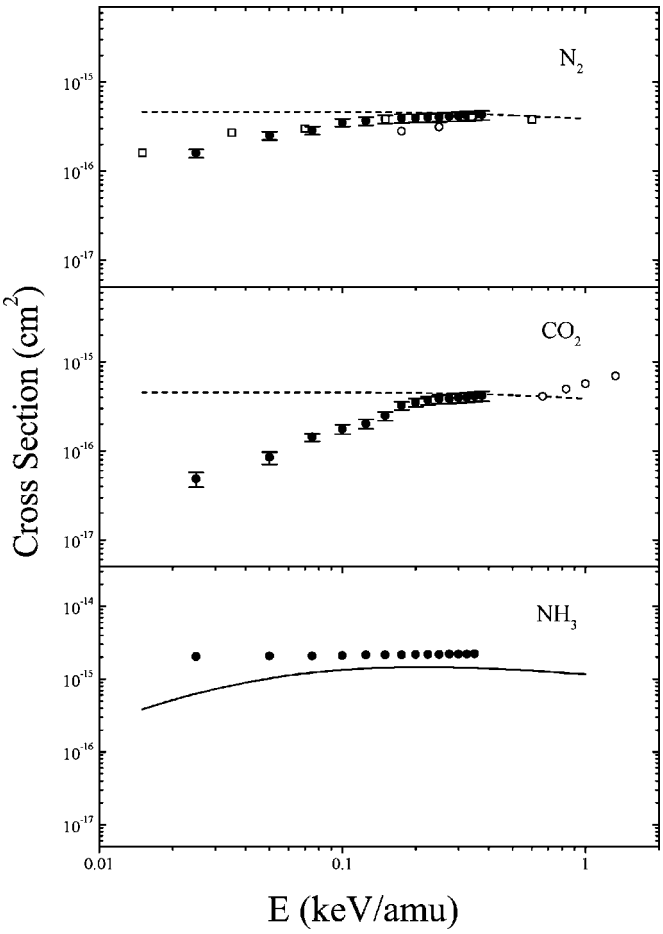

FIG. 5. Total cross sections for single-electron capture by He^{2+} ions from N_2, CO_2, and NH_3. ●, present work. Theory: solid lines, Demkov model; dashed lines, LZ model. ○, Hanaki *et al.* [10]; □, Ishii *et al.* [13]; △, Greenwood *et al.* [14].

C. $He^{2+}+N_2$ collisions

Figure 4(b) shows the translational energy-gain spectra for the formation of He^+ ions from the reaction of 100 eV He^{2+} ions with N_2 at 0° scattering angles. The spectrum shows only one broad peak at about $Q \approx 10$ eV; this peak correlates with DTI. As the scattering angle is increased, dissociative transfer ionization channel remains dominant, but the relative importance of reaction channels due to the formation of N_2^{2+} ions into higher excited states with possible dissociation into $N^+(3P)+N^+(3P)$ increases [29], which shown as a long tail at $Q \leqslant 7$ eV. Furthermore, the DTI process is the dominant reaction channel observed over the entire collision energy region studied, in agreement with the other measurements [5,6].

The measured total cross sections for single-electron capture by He^{2+} ions from N_2 as a function of the collision energy are shown in Fig. 5, together with other available measurements and cross sections calculated using the Landau-Zener model. The present measurements are somewhat larger than the results of Hanaki *et al.* [10] and in good agreement with the experimental results of Ishii *et al.* [13], and show similar behavior; cross sections slowly increase with increasing impact energies. This can be understood from the reaction window, which gets broader with increasing impact energies and therefore capture channels with smaller and larger Q values get an increasing probability. As can also be seen, for impact energies $E \geqslant 0.1$ keV/amu, our data are in good agreement with the results of the Landau-Zener model, but the model overestimates the cross sections at lower energies. The calculations show that mechanism for the formation of dissociative transfer ionization channel involves an exothermic two-electron process driven by the electron-electron interaction.

D. $He^{2+}+CO_2$ collisions

Figure 4(c) shows the translational energy-gain spectra observed for the formation of He^+ from the reaction of He^{2+} ions with CO_2 at 0° scattering angle and collision energy of 200 eV. The observed spectra clearly indicate that dissociative transfer ionization, due to single-electron capture into the $n=1$ state of He^+ ions accompanied by ionization of the molecular target ion, is predominant over the entire impact energy region studied via the reaction channel

$$He^{2+} + CO_2 \rightarrow He^+(n=1) + {CO_2}^{2+} + e + Q(=10\ \text{eV}).$$

With an energy gain of about 10 eV, the accessible states of ${CO_2}^{2+}$ may correspond to several singlet and triplet Σ, Π, and Δ states of $4\sigma_g^{-1}$, $1\pi_g^{-1}$, and $1\pi_u^{-2}$ configurations whose calculated energies lie between 42.9 and 44 eV. These states may dissociate into $O^+ + CO^+$ products [30].

As the projectile impact energy is increased, the dissociative transfer ionization channel remains dominant, but a long tail on the lower-energy side of the dominant channel was observed. This is attributed to the formation of ${CO_2}^{2+}$ ions into higher excited states with possible dissociation into $C^+ + O^+ + O$ [31]. These states were also detected at larger projectile scattering angles [15]. No other experimental data are available for comparison.

Total cross sections for He^{2+} ions colliding with CO_2 in the collision energy range 0.025–0.4 keV/amu are presented in Fig. 5, together with the results of Greenwood *et al.* [14] at higher energies and are compared with Landau-Zener calculations. As can be seen, the total cross sections slowly increase with increasing impact energies and show very little dependence on collision energy above 0.2 keV/amu. This can also be understood from the reaction window, which gets broader with increasing impact energies and therefore capture channels with larger or smaller Q values increase in probability. Our cross sections are in excellent agreement with the results of the Landau-Zener model at high energies but show a discrepancy below collision energies of 0.2 keV/amu. The model indicates that dissociatative transfer ionization process is produced by an electron-electron interaction. There are no previous data for single-electron capture cross sections for He^{2+} on CO_2 in this energy range. However, the lower-energy work of Greenwood *et al.* [14] appears to extrapolate well to our data.

IV. CONCLUSIONS

We have used translational energy-gain spectroscopy to measure doubly differential cross sections for single-electron

capture by He^{2+} ions from NH_3, N_2, O_2, and CO_2 at collision energies between 0.025 and 0.400 keV/amu and at laboratory scattering angles between 0° and 8°. Translational energy gain spectra for single-electron capture by He^{2+} ions from NH_3 indicated that the populations of the intermediate vibrational levels dominate at forward scattering angles and the relative importance of lower vibrational levels is increased with increasing impact energy. For the N_2 and CO_2 targets, dissociative transfer ionization is the dominant channel observed over the entire collision energy region studied. In addition, a long tail at a low-energy gain side of the peak has been observed; this might include capture with dissociation into the single-charged ions. It is noticeable that the peaks for dissociative transfer ionization processes are broader than those for nondissociative single-electron capture. This is, of course, due to a much larger number of exit channels contributing to the DTI including excited states of the product ions.

The energy dependence of the absolute state-selective and total cross sections for single-electron capture by He^{2+} ions from O_2, CO_2, N_2, and NH_3 of the present work were compared with the available data and the theoretical calculations based on the Demkov and Landau-Zener models. Our measured state-selective cross sections for the O_2 target have been shown to be in reasonable agreement with the calculated cross sections. In addition, our present total cross sections for this system show good agreement with other available data. For He^{2+} on N_2 and CO_2 collisions, the energy dependence of the experimental values is reproduced, at least qualitatively, by Landau-Zener calculations and shows good agreement with other available data. For He^{2+} on NH_3, the cross sections are almost independent of the collision energies and can be understood from the reaction window. Finally, the calculations show that the mechanism for DTI involves two electron-transfer processes driven by electron-electron interaction, whereas the nondissociative SEC processes are induced by the nucleus-electron interaction.

[1] S. Steigman, Astrophys. **199**, 642 (1975).
[2] D. Pequignot, Astron. Astrophys. **81**, 356 (1981).
[3] V. A. Krasnipolsky, M. J. Mumma, M. Abbott, B. C. Flynn, K. J. Meech, D. K. Yeomans, P. D. Feldman, and C. B. Cosmovici, Science **277**, 1488 (1997).
[4] W. T. Rogers, J. W. Boring, and R. E. Johnson, J. Phys. B **11**, 2319 (1978).
[5] N. Kobayashi, T. Iwai, Y. Kaneko, M. Kimura, A. Matsumoto, S. Ohtani, K. Okuno, S. Takagi, H. Tawara, and S. Tsurubuchi, J. Phys. Soc. Jpn. **53**, 3736 (1984).
[6] S. J. Martin, J. Stevens, and E. Pollack, Phys. Rev. A **43**, 3503 (1991).
[7] M. Fárnīk, Z. Herman, T. Ruhaltinger, and J. Peter Tooennies, J. Chem. Phys. **103**, 3495 (1995).
[8] R. W. McCullough, T. K. McLaughlin, T. Koizumi, and H. B. Gilbody, J. Phys. B **25**, L193 (1992).
[9] M. Albu, F. Aumayr, and H. Winter, Int. J. Mass. Spectrom. **233**, 239 (2004).
[10] H. Hanaki, T. Kusakabe, N. Nagai, and M. Sakisaka, J. Phys. Soc. Jpn. **52**, 424 (1983).
[11] M. E. Rudd, T. V. Goffe, and A. Itoh, Phys. Rev. A **32**, 2128 (1985).
[12] W. R. Thompson, M. B. Shah, and H. B. Gilbody, Phys. Scr. **T73**, 215 (1997).
[13] K. Ishii, K. Okuno, and N. Kobayashi, Phys. Scr. **T80**, 376 (1999).
[14] J. B. Greenwood, A. Chutjian, and S. J. Smith, Astrophys. **529**, 605 (2000).
[15] O. Abu-Haija, E. Y. Kamber, and S. M. Ferguson, Nucl. Instrum. Methods Phys. Res. B **205**, 634 (2003).
[16] B. Seredyuk, R. W. McCullough, H. Tawara, H. B. Gilbody, D. Bodewits, R. Hoekstra, A. G. G. M. Tielens, P. Sobocinski, D. Pesic, R. Hellhammer, B. Sulik, N. Stolterfoht, O. Abu-Haija, and E. Y. Kamber, Phys. Rev. A **71**, 022705 (2005).
[17] E. Y. Kamber, O. Abu-Haija, and S. M. Ferguson, Phys. Rev. A **65**, 062717 (2002).
[18] S. Yaltkaya, E. Y. Kamber, and S. M. Ferguson, Phys. Rev. A **48**, 382 (1993).
[19] *Collision Spectroscopy*, edited by R. G. Cooks (Plenum, New York, 1978), p. 252.
[20] C. E. Moore, *Atomic Energy Levels*, Natl. Bur. Stand. (U.S.) Circ. No. 467 (U.S. GPO, Washington, D.C., 1970).
[21] R. D. Levin and S. G. Lias, *Ionization Potential and Appearance Potential Measurements 1971–1981*, Natl. Bur. Stand. Ref. Data Ser. Natl. Bur. Stand. (U.S.) Circ. No. 71 (U.S. GPO, Washington, D.C., 1982).
[22] Y. N. Demkov, Zh. Eksp. Teor. Fiz. **45**, 195 (1963) [Sov. Phys. JETP **18**, 138 (1964)].
[23] L. D. Landau, Phys. Z. Sowjetunion **2**, 46 (1932).
[24] C. Zener, Proc. R. Soc. London, Ser. A **137**, 696 (1932).
[25] R. E. Oslon and A. Salop, Phys. Rev. A **14**, 579 (1976).
[26] N. Stolterfoht, in *Progress in Atomic Spectroscopy*, edited by H. Kleinoppen (Plenum Press, New York, 1987), Part D, p. 415.
[27] N. Stolterfoht, Phys. Rev. A **47**, R763 (1993).
[28] H. Ågren, I. Reineck, H. Veenhuizen, R. Maripuu, R. Arneberg, and L. Karlsson, Mol. Phys. **45**, 477 (1982).
[29] J. M. Curtis and R. K. Boyd, J. Chem. Phys. **81**, 2991 (1984).
[30] P. Millie, I. Nenner, P. Archirel, P. Lablanquie, P. Fournier, J. H. D., and J. Eland, Chem. Phys. **84**, 1259 (1986).
[31] T. Masuoka, E. Nakamura, and A. Hiraya, J. Chem. Phys. **104**, 6200 (1996).